

Role of Ice Dynamics in the Sea Ice Mass Balance

PAGES 515–516

Over the past decade, the Arctic Ocean and Beaufort Sea ice pack has been less extensive and thinner than has been observed during the previous 35 years [e.g., *Wadhams and Davis*, 2000; *Tucker et al.*, 2001; *Rothrock et al.*, 1999; *Parkinson and Cavalieri*, 2002; *Comiso*, 2002]. During the summers of 2007 and 2008, the ice extents for both the Beaufort Sea and the Northern Hemisphere were the lowest on record. Mechanisms causing recent sea ice change in the Pacific Arctic and the Beaufort Sea are under investigation on many fronts [e.g., *Drobot and Maslanik*, 2003; *Shimada et al.*, 2006]; the mechanisms include increased ocean surface warming due to Pacific Ocean water inflow to the region and variability in meteorological and surface conditions. However, in most studies addressing these events, the impact of sea ice dynamics, specifically deformation, has not been measured in detail.

The aim of the Sea Ice Experiment: Dynamic Nature of the Arctic (SEDNA) project is to improve understanding of the processes leading to changes in the distribution of sea ice thickness as a function of mechanical processes and spatial scaling. For phase 1 of the SEDNA project, an international team of researchers spent 2 weeks in April 2007 on the sea ice of the Beaufort Sea deploying an extensive ensemble of drifting buoys and collecting in situ and satellite data. The goal of the project was to measure the contribution of sea ice dynamics to the observed reduction of sea ice in the Beaufort Sea and the Arctic Ocean.

Coordinating Observations

Understanding the impact of ice dynamics on sea ice mass balance requires an accurate representation of how mechanics and thermodynamics relate to variability in boundary forces on the ice pack. Ice growth, melt, advection, and deformation control changes in sea ice thickness distribution. Ice growth and melt rates are highly variable, due to meter-scale ice thickness and snow cover heterogeneity and oceanic and meteorological conditions. Meter-scale spatial heterogeneity is controlled by the superposition of a thermodynamic response on an ice-scape sculpted by mechanical redistribution of ice thickness. Mechanical deformation occurs abruptly, predominantly in winter, causing linearly organized regions of deformation (leads and ridges).

Recent technological developments support revisiting the empirical scaling relationships between sea ice stress, strain rate, and redistribution with measurement precision not previously possible. The ice thickness distribution can be measured with satellite altimetry (SA) of sea ice freeboard (the distance between ice top surface and

ocean); airborne electromagnetic induction with single-beam laser altimetry (EM-bird); surface electromagnetic induction (EMI); and airborne laser scanner (lidar). Improvements in autonomous buoys (GPS-increased accuracy, autonomous stress sensors) and synthetic aperture radar (SAR) ice motion analysis allow better identification of pack stress/strain rate relations.

Experimental Design

SEDNA is a highly coordinated effort to directly observe pack ice stress, strain rate, and redistribution on scales ranging from 10 kilometers to the entire Beaufort Sea.

We wished to monitor the dynamic evolution of the ice pack, which is manifest in cracking, lead opening and shearing, ridge building when cracks and leads close, and the effect of lead opening on the growth of new ice. Concurrent in situ and remote observations limit error and allow intercomparison between different measurements of the same parameter over a range of spatial scales. Our measurement ensemble during phase 1 of SEDNA was designed to resolve two key processes in the dynamic evolution of sea ice: (1) the relationship between pack ice stress, strain rate, and failure, manifest in cracking and the subsequent opening and closing of leads (fractures in the pack that can be meters to kilometers wide); and (2) the

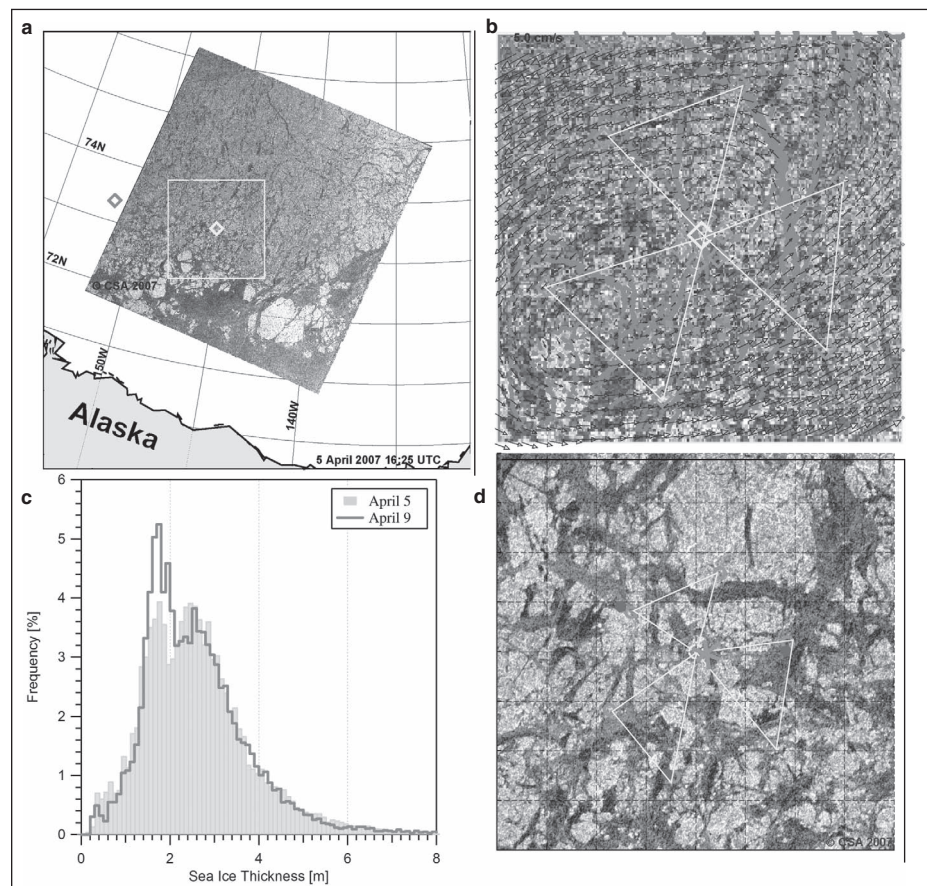


Fig. 1. (a) The Sea Ice Experiment: Dynamic Nature of the Arctic (SEDNA) array on 5 April 2007, showing buoy positions overlaid on a RADARSAT ScanSAR B scene (red diamonds, meteorological beacons; green diamonds, GPS drifters; yellow diamond, the Applied Physics Laboratory ice camp with ice mass balance buoy and two stress sensors). (b) Enlargement of the region within the yellow box in Figure 1a, showing an outer (70-kilometer radius) and inner (10-kilometer radius) buoy array of GPS drifters (green diamonds). Ice motion vectors are plotted every 6.4 kilometers. The continuous series of red dots, which appear as red lines, show discontinuities in ice motion field, calculated between two synthetic aperture radar (SAR) images on 5 and 8 April 2007. Green squares are GPS drifters clustered in groups along individual leads. (c) Ice thickness distribution, estimated by airborne electromagnetic induction with single beam laser altimetry for 5 and 9 April 2007, captures change due to deformation. (d) Enlargement of the central region of Figure 1b, centered on the yellow square, without ice drift vectors and discontinuities plotted, showing the inner, 10-kilometer-radius buoy array (green circles). Blue dots are stress buoys. Light detection and ranging (not shown) and electromagnetic induction (yellow lines) aerial surveys of ice thickness were performed over the two scales. A submarine-based upward looking sonar survey of the 10-kilometer region is not shown. One-kilometer calibration transects (the green lines forming the asterisk) and a detailed ridge study allow for the intercomparison of all thickness measurements. The yellow circle is the location of the ice camp. Original color image appears at the back of this volume.

evolution of the ice thickness distribution, separating out dynamic from thermodynamic changes.

GPS-located drifting buoys provide good temporal resolution of strain rate but offer limited spatial representation, whereas SAR motion vector analysis provides excellent spatial coverage but poor temporal resolution. Combining these two data sets resolves sea ice deformation over the scales that it is known to affect sea ice mass balance. No single ice thickness measurement method can fully resolve the ice thickness distribution over the scales of interest, from 1 kilometer to the Arctic Basin.

To resolve dynamic changes in the thickness distribution, we coordinated airborne and surface electromagnetic induction ice thickness measurements, airborne laser altimeter retrievals, submarine and autonomous underwater vehicle upward looking sonar (ULS) swaths, and direct measurements. Recent SA developments could provide basin-wide sea ice thickness estimates, overcoming spatial and temporal limitations of other methods (such as thickness estimates from in situ, moored, airborne, and submarine-borne instrumentation). However, this requires knowledge of snow depth and density [Giles *et al.*, 2007]. The snow data we collected during phase 1 of SEDNA are useful for the conversion of SA sea ice freeboard to thickness. SA thickness estimates, from the European Space Agency's Envisat radar altimetry and NASA's ICESat laser altimetry, extend SEDNA ice thickness data to the entire Arctic Ocean. Figure 1 illustrates how observations have been coordinated with nested buoy arrays and satellite data.

Buoy and satellite data, collected throughout 2007, allow for the investigation of changes in the mechanical properties of pack ice over the winter to summer transition. During late winter (April), coherence in pack ice deformation over 70 kilometers indicates effective stress propagation through the ice pack. Deformation over 70-kilometer scales becomes uncorrelated in early May. We observe a temporally sharp transition from a connected winter pack

ice to spring breakup, when the mechanism for stress transfer through the ice pack changes.

The SEDNA field campaign was designed to validate Arctic sea ice models and provide information for developing future Arctic pack ice monitoring networks. Verifying that models reproduce observed influences of ice dynamics on ice thickness is essential for representing dynamic-thermodynamic feedbacks within climate models. SEDNA data will be publicly available by 2010, after the end of the International Polar Year.

Acknowledgments

This research was funded by the U.S. National Science Foundation (grants NSF ARC 0612527, 0612105, 0611991, and 0612402). The U.S. Navy's Arctic Submarine Laboratory provided access to the Applied Physics Laboratory (APL) Ice Station 2007 (APLIS07). Thanks to Fred Karig and the APL team who ran APLIS07. The Alaska Satellite Facility (ASF) of the Geophysical Institute of the University of Alaska Fairbanks (especially Melanie Engram of ASF) and the National Ice Center of the U.S. National Oceanic and Atmospheric Administration (NOAA) facilitated near-real-time transfer of RADARSAT 1 ScanSAR-B imagery provided by the Canadian Space Agency. NASA and ASF provided a full year of SAR data covering the entire Beaufort Sea. The European Union's DAMOCLES project sponsored airborne lidar measurements. The International Arctic Buoy Program archives SEDNA buoy data and provided three meteorological buoys.

References

- Comiso, J. C. (2002), A rapidly declining perennial sea ice cover in the Arctic, *Geophys. Res. Lett.*, *29*(20), 1956, doi:10.2929/2002GL015650.
- Drobot, S. D., and J. A. Maslanik (2003), Interannual variability in summer Beaufort Sea ice conditions: Relationship to winter and summer surface and atmospheric variability, *J. Geophys. Res.*, *108*(C7), 3233, doi:10.1029/2002JC001537.
- Giles, K. A., S. W. Laxon, and A. P. Worby (2008), Antarctic sea ice elevation from satellite

radar altimetry, *Geophys. Res. Lett.*, *35*, L03503, doi:10.1029/2007GL031572.

- Parkinson, C. L., and D. J. Cavalieri (2002), A 21-year record of Arctic sea-ice extents and their regional, seasonal and monthly variability and trends, *Ann. Glaciol.*, *34*, 441–446.
- Rothrock, D. A., Y. Yu, and G. A. Maykut (1999), Thinning of the Arctic sea ice cover, *Geophys. Res. Lett.*, *26*(23), 3469–3472.
- Shimada, K., T. Kamoshida, M. Itoh, S. Nishino, E. Carmack, F. McLaughlin, S. Zimmerman, and A. Proshutinsky (2006), Pacific Ocean inflow: Influence on catastrophic reduction of sea ice cover in the Arctic Ocean, *Geophys. Res. Lett.*, *33*, L08605, doi:10.1029/2006GL025624.
- Tucker, W. B., III, J. W. Weatherly, D. T. Eppler, L. D. Farmer, and D. L. Bentley (2001), Evidence for rapid thinning of sea ice in the western Arctic Ocean at the end of the 1980s, *Geophys. Res. Lett.*, *28*(14), 2851–2854.
- Wadhams, P., and N. R. Davis (2000), Further evidence of ice thinning in the Arctic Ocean, *Geophys. Res. Lett.*, *27*(24), 3973–3975.

—JENNIFER HUTCHINGS, International Arctic Research Center, University of Alaska Fairbanks (UAF); E-mail: jenny@iarc.uaf.edu; CATHLEEN GEIGER, Department of Geography, University of Delaware, Newark; ANDREW ROBERTS, Arctic Region Supercomputing Center and International Arctic Research Center, UAF; JACQUELINE RICHTER-MENGE, Cold Regions Research and Engineering Laboratory, U.S. Army Corps of Engineers, Hanover, N. H.; MARTIN DOBLE, Department of Applied Mathematics and Theoretical Physics (DAMTP), University of Cambridge, Cambridge, UK; RENE FORSBERG, Danish National Space Center, Copenhagen, Denmark; KATHARINE GILES, Centre for Polar Observation and Modelling (CPOM), University College London; CHRISTIAN HAAS, Earth and Atmospheric Sciences, University of Alberta, Edmonton, Canada; STEFAN HENDRICKS, Alfred Wegener Institute for Polar and Marine Research, Bremerhaven, Germany; CHANDRA KHAMBHAMETTU, Video Image Modeling and Synthesis Laboratory, University of Delaware; SEYMOUR LAXON, CPOM; TORGE MARTIN, NOAA Geophysical Fluid Dynamics Laboratory, Princeton, N. J.; MATTHEW PRUIS, NorthWest Research Associates, Seattle, Wash.; MANI THOMAS, Video Image Modeling and Synthesis Laboratory, University of Delaware; PETER WADHAMS, DAMTP; and H. JAY ZWALLY, NASA Goddard Space Flight Center, Greenbelt, Md.

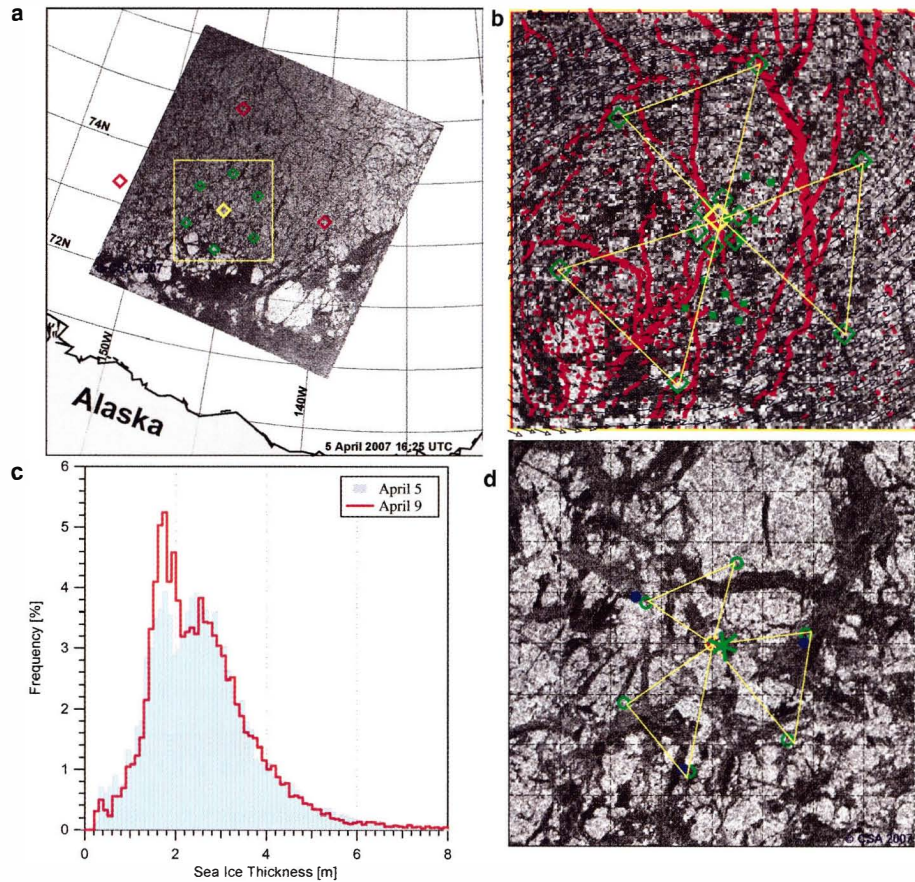


Fig. 1. (a) The Sea Ice Experiment: Dynamic Nature of the Arctic (SEDNA) array on 5 April 2007, showing buoy positions overlaid on a RADARSAT ScanSAR B scene (red diamonds, meteorological beacons; green diamonds, GPS drifters; yellow diamond, the Applied Physics Laboratory ice camp with ice mass balance buoy and two stress sensors). (b) Enlargement of the region within the yellow box in Figure 1a, showing an outer (70-kilometer radius) and inner (10-kilometer radius) buoy array of GPS drifters (green diamonds). Ice motion vectors are plotted every 6.4 kilometers. The continuous series of red dots, which appear as red lines, show discontinuities in ice motion field, calculated between two synthetic aperture radar (SAR) images on 5 and 8 April 2007. Green squares are GPS drifters clustered in groups along individual leads. (c) Ice thickness distribution, estimated by airborne electromagnetic induction with single beam laser altimetry for 5 and 9 April 2007, captures change due to deformation. (d) Enlargement of the central region of Figure 1b, centered on the yellow square, without ice drift vectors and discontinuities plotted, showing the inner, 10-kilometer-radius buoy array (green circles). Blue dots are stress buoys. Light detection and ranging (not shown) and electromagnetic induction (yellow lines) aerial surveys of ice thickness were performed over the two scales. A submarine-based upward looking sonar survey of the 10-kilometer region is not shown. One-kilometer calibration transects (the green lines forming the asterisk) and a detailed ridge study allow for the intercomparison of all thickness measurements. The yellow circle is the location of the ice camp.